Growth of the Cr oxides via activated oxygen reactive molecular beam epitaxy: Comparison of the Mo and W oxides

N. J. C. Ingle,[a] R. H. Hammond, and M. R. Beasley
Department of Applied Physics, Stanford University, Stanford, California 94305

(Received 11 August 2000; accepted for publication 22 January 2001)

The realization of spin polarized tunnel devices made with CrO_2, a theorized half-metallic ferromagnet, requires stringent control of surface and interface quality ideally obtainable via molecular beam epitaxy (MBE) growth. We have studied the MBE growth of all the di- and tri-oxides of the group VIB transition metals (Cr, Mo, and W), with the aid of a high flux atomic oxygen source and detection scheme, to help understand which oxidation states are reachable. We find that even though we can reach the $+6$ oxidation state of Cr (CrO_3) we are unable to obtain single phase CrO_2, the $+4$ oxidation state. One interpretation of our results is that the physical effect of pressure, not solely the oxidation potential, is important to the growth of single phase CrO_2. [DOI: 10.1063/1.1355286]

I. INTRODUCTION

Many articles in the last couple of years have suggested CrO_2 may be an ideal material to use in giant magnetoresistance spin valves and spin dependent tunnel junction devices due to its theoretical 100% spin polarization or half-metallic ferromagnetism.[1–6] For its use in these types of devices, a high quality multilayer structure must be grown. One such structure would be the epitaxial layering of CrO_2 and TiO_2, where TiO_2 would be used as an insulating barrier.

To date, there are two methods to produce CrO_2 films. Both involve the decomposition of CrO_3 under at least an atmosphere pressure of oxygen gas, while neither typically produces surfaces that would allow the aforementioned devices to be fabricated. DeVries[7] and more recently Ranno *et al.*[8] produced their films by placing a TiO_2 substrate and CrO_3 powder in a sealed reactor. By controlled heating they were able to decompose the CrO_3 powder into CrO_2, which forms a highly textured thick film on the TiO_2 substrates; the pressure of the reactor when complete decomposition into CrO_2 has occurred is about 800 bar. Originally Ishibashi *et al.*[9,10] and more recently Suzuki and Tedrow[11] and Li *et al.*[12,13] used a simple two-zone atmospheric pressure CVD growth method where the CrO_3 is heated in one zone of the chamber and atmospheric pressure O_2 is used as a carrier gas to transport the sublimed CrO_3 over to a second zone held at a higher temperature containing a TiO_2 substrate.

The type of high quality interfaces and epitaxial layering required to maximize the effect of the 100% spin polarization in tunnel junctions is more often associated with molecular beam epitaxial (MBE) growth than with the previously mentioned film growth techniques. Barry *et al.*[14] have shown that the samples made via the high pressure reactor method[8] are not easily used to fabricate tunnel junctions that allow the extraction of spin polarization information, or that can be made into useful magnetoresistive devices. The reason for this could have as much to do with poor, uncontrolled interfaces as with the suggested fact that the native barrier Cr_2O_3, an antiferromagnet, is not an appropriate choice for a tunneling barrier in a spin-dependent tunneling device.

In this article we study the possible MBE growth of CrO_2 with thermally evaporated Cr and a source of activated oxygen, and more generally, the concept of using low pressures of activated oxygen as the driving force for oxidation reactions in lieu of high pressures of molecular oxygen. The thermodynamic and kinetic aspects of using activated oxygen in place of higher pressure so molecular oxygen will be discussed in a subsequent article. We compare here the growth of the Cr oxides with that of the other group VIB elements, Mo and W, to obtain a clearer picture of which oxidation levels are reachable via our MBE growth conditions. We also study the effect of epitaxially matched substrates on the growth on the various oxidation states of Cr, Mo, and W.

II. EXPERIMENT

The thermal evaporation of Cr with MBE compatible pressures (up to 1×10^{-4} Torr) of molecular oxygen O_2 will always produce films with a Cr oxidation state of $+3$, i.e., Cr_2O_3. In order to reach higher oxidations states (that of $+4$ and $+6$ associated with CrO_2 and CrO_3, respectively), a source of active oxygen must be used. For this work we used a flow-through microwave plasma source of atomic oxygen. An atomic absorption detection scheme was used to measure fluxes of up to 1×10^{18} atoms/cm^2 s of atomic oxygen. This flux is about 2 orders of magnitude higher than any previously published data for atomic oxygen sources. The equivalent atomic oxygen partial pressure at the substrate, calculated from this maximum flux, is 2 mTorr. This atomic oxygen source and detection scheme has been described in detail elsewhere.[15]

Reflection high energy electron diffraction (RHEED) was performed during growth and was primarily used to de-

[a]Author to whom correspondence should be addressed; electronic mail: ingle@loki.stanford.edu

termine the long range ordering of the structure. In interpreting the data, the classic streaky RHEED pattern or a three dimensional spotty pattern was taken to indicate epitaxial film growth, strong rings as polycrystalline growth, and a diffuse uniform background as amorphous film growth.

The oxidation state of the transition metals was determined by observing the chemical shifts of core-level photoemission. The x-ray photoemission (XPS) spectra were measured in an *in situ* VG ESCALAB Mark 2 spectrometer equipped with a twin anode x-ray source. All XPS data shown in this article have had spectral components associated with the $K_{\alpha_{3,4}}$ x-ray satellites subtracted and then a Shirley-style[16] background removed. No contaminants such as carbon were seen in the spectra. This absence of carbon allows all O to be associated with the transition metal oxide, and therefore all chemical shifts in the transition metal can be associated with the films oxygen environment. It is also worth noting that there is no model fitting needed to extract the oxidation state from core level XPS.

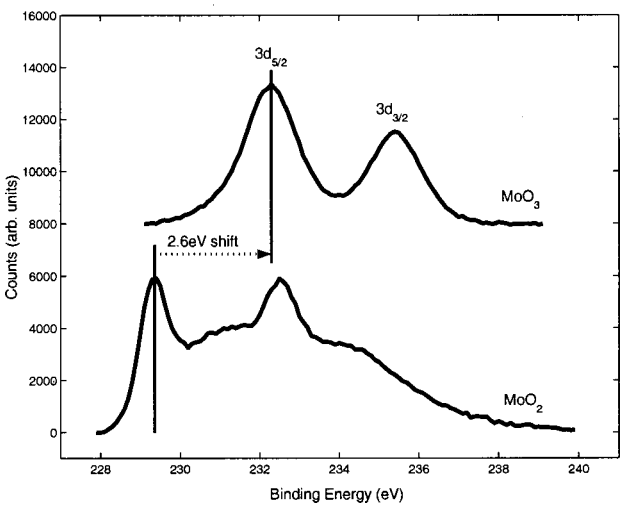

FIG. 1. Mo $3d$ *in situ* core level x-ray photoemission indicating the chemical shift due to the oxidation state.

III. RESULTS AND DISCUSSIONS

Cr, Mo, and W, the group VIB transition metals, all form di- and trioxides. CrO_2, MoO_2, and WO_2 form a chemically and structurally similar series of metallic oxides. All three have the rutile (TiO_2) structure with very similar unit cell sizes, and all three show good metallic conductivity; however MoO_2 and WO_2 do not show interesting magnetic properties. CrO_3, MoO_3, and WO_3 are not normally considered a series due to the structural difference between them. The Cr in CrO_3 [space group $C_{2v}^{16}(Ama)$] is centered in a tetrahedral oxygen environment, while the Mo and W in MoO_3 and WO_3 are centered in an octahedral oxygen coordination which are then arranged in a distorted ReO_3-type structure. As with the dioxide series the electrical properties of the trioxides are the same, while their magnetic properties differ. MoO_2 and WO_3 show the diamagnetism expected for a closed shell insulator, while CrO_3 is paramagnetic,[17] but nominally still a closed shell insulator.

Due to the simplicity of the growth of Mo and W oxides we shall discuss these first and then make a comparison to the growth of the Cr oxides. Figures 1 and 2 show the *in situ* core level XPS for Mo and W, respectively, in the two possible oxidation states. The upper curve in Fig. 1 shows the Mo $3d$ core level peaks at 232.2 and 235.5 eV. These are very symmetric peaks and are similar to those found in the literature in terms of absolute energy position (relative to the O $1s$ peaks[18]) and overall shape for Mo in a MoO_3 environment. The lower curve shows the same Mo $3d$ core level peaks for Mo in a MoO_2 environment. In several works[19,20] the peak shape of the Mo $3d$ core levels in MoO_2 was believed to be due to multiple oxidation states being present. However, others[21,22] have suggested the extended shape on the higher binding energy side is due to the interaction between the produced core level hole and the conduction electrons. We believe the latter is the case and that we do not have multiple oxidation states in the sample. Experimentally, we measure exactly the same spectra for samples grown under a large range of different oxidation potentials. If the extra spectral weight was due to mixed oxidation states the relative heights of the various oxidation states should shift with changing oxidation potential which we do not see.

Figure 2 shows a very similar set of curves for W. These curves are for the $4f$ core levels of W, where the upper curve shows W in a WO_3 environment and the lower curve shows W in a WO_2 environment. Again, we see the spreading of spectral weight over higher binding energies from the WO_2 sample. This is a very distinct fingerprint of a narrow conduction band metallic oxide phase being present. The strongly opaque and reflective properties the film possesses when looked at with the naked eye are also consistent with the film being a metallic oxide.

Figures 3 and 4 show the Mo–O and W–O temperature–oxygen potential ''phase'' diagram as empirically determined from our chamber. The vertical axis is explained below. The oxidation state of the Mo or W shown in these diagrams is determined via *in situ* core level XPS as

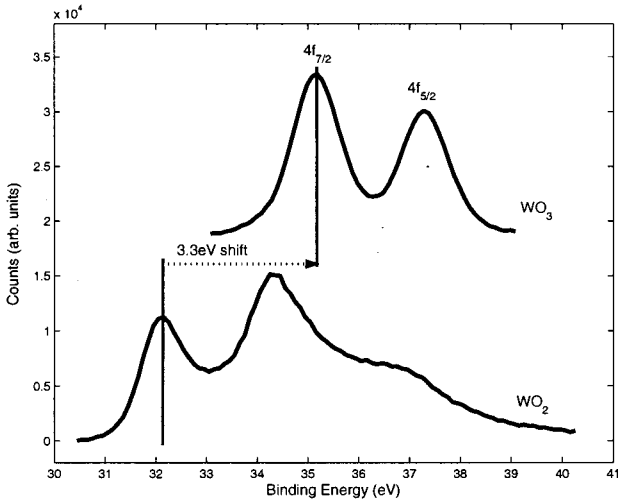

FIG. 2. W $4f$ *in situ* core level x-ray photoemission indicating the chemical shift due to the oxidation state.

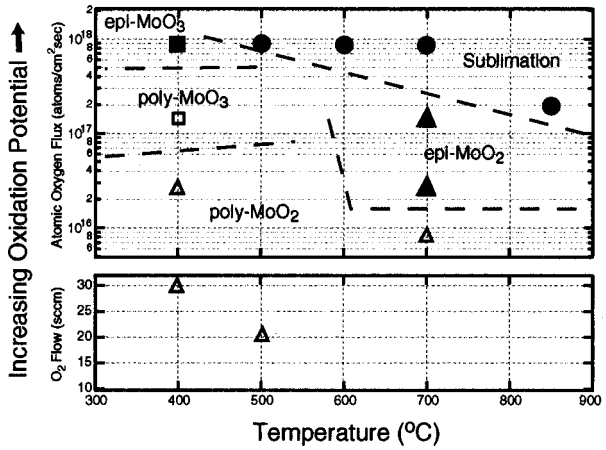

FIG. 3. The empirically determined Mo–O phase diagram. Different symbols are used to group data points according to growth morphology (epi =epitaxial, poly=polycrystalline) and oxidation state.

discussed above, while the growth morphology of the film, either polycrystalline or epitaxial (single crystal-like) is observed via RHEED. Groups of data points on these phase diagrams showing different growth morphology and oxidation states are given different symbols which define specific regions within the diagram. The lines separating these different regions in the phase diagram are only intended as rough indicators of a change in oxidation state or growth morphology as the oxidation potential or temperature are altered in a particular direction.

The vertical axis of these phase diagrams is intended as a general indicator of increasing oxidation potential. It is split into the two parameters most easily measured while growing oxide films. Specifically, the flow of molecular oxygen (proportional to the overall chamber pressure) is used when growing with molecular oxygen, and the flux of atomic oxygen (at roughly constant overall chamber pressure) when growing with atomic oxygen. The atomic oxygen flux axis sits above the flow of molecular oxygen axis because it is generally believed that atomic oxygen has a higher oxidation potential than molecular oxygen. The exact connection between the two axes is determined either by thermodynamics or kinetics depending on the reactions occurring. This admittedly subtle matter will be covered in more detail in a later article.

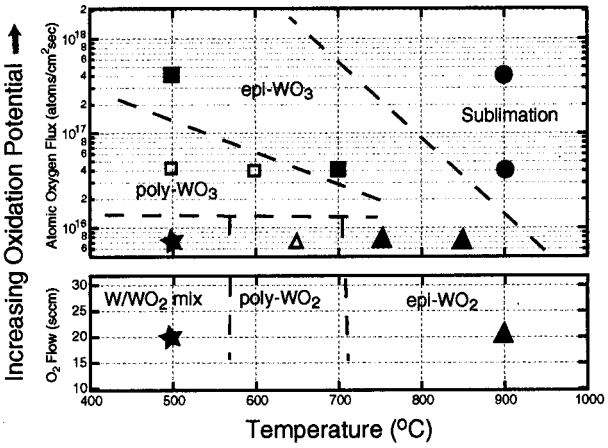

FIG. 4. The empirically determined W–O phase diagram. Different symbols are used to group data points according to growth morphology (epi =epitaxial, poly=polycrystalline) and oxidation state.

The minimum amount of oxygen needed to form the desired phases is determined by the stoichiometry of the intended phase and the rate at which the transition metal is deposited. In this article the deposition rate of the transition metals was held roughly constant between 0.5 and 1 Å/s, corresponding to a flux of $\approx 1\times 10^{14}$ atoms/cm s. A flow rate of roughly 0.3 sccm of molecular oxygen is all that is needed to have the stoichiometrically required amount of oxygen. Hence, all of the films are grown in an oxygen regime well above the stoichiometric needs of even the highest oxidized phases.

The first region of importance in Figs. 3 and 4, and one of the features that is common to the phase diagrams for Mo, W, and Cr, is the ''sublimation'' region. In this region of temperature and oxidation potential, regardless of the growth time, XPS shows a strong signal from the substrate, and only a very small signal from the transition metal. The chemical shift in the transition metal core level indicates that what does stick is in the +6 oxidation state (i.e., MoO_3 or WO_3). This suggests that under these conditions sublimation of the trioxide is occurring, and that it is not a matter of the sticking coefficient to the substrate dropping close to zero.

In both the empirical Mo and W phase diagrams the change from one oxidation state to the next as temperature or oxidation potential is changed is abrupt. There are no regions where both the +4 and +6 oxidation states are found with varying ratios as the temperature or oxidation potential is varied. In the W–O phase diagram a region at the lowest temperature and oxidation potential does show a mix of unoxidized W and WO_2. Also noteworthy in both the Mo and W diagrams is the fact that the conditions under which epitaxial growth occurs is adjacent to the sublimation region.

On a more general note, the Mo–O phase diagram looks like a subset of the W–O phase diagram with the temperature and oxidation potential axes scaled. The lower edge of the sublimation region shifts down in temperature and the amount of oxidation potential needed to form the oxides increases. The direction of scaling for both the temperature and oxidation potential are expected from the thermodynamic phase diagrams,[23] calculated thermodynamic phase stability limits,[24] and the relationship between melting temperatures of the trioxides. Furthermore, as one moves up the group VIB column of the periodic table to Cr, the temperature scale is expected to continue to decrease and the oxidation potential needed to form the oxides increase. This means that for W a larger portion of phase space can be studied because the upper temperature boundary is higher, while the lower boundary, which is set by kinetic issues with growth, is similar for all materials. Following this logic, we would expect the Cr–O phase diagram to be an appropriately scaled subset of the Mo–O phase diagram and due to the lower temperatures involved, the kinetic limitations on growth to be more pronounced.

Figure 5 shows the Cr–O temperature–oxygen potential phase diagram as empirically determined from our chamber

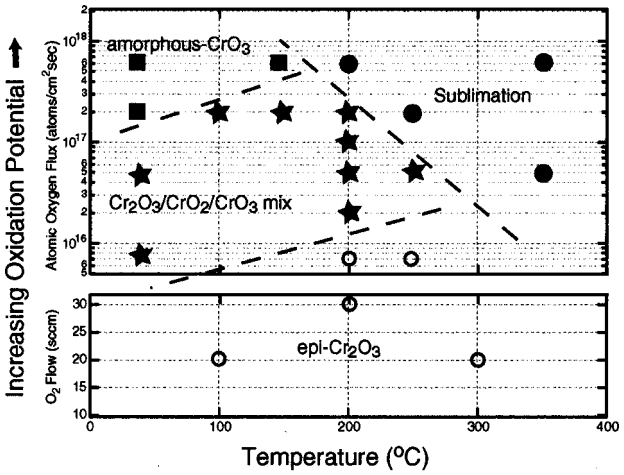

FIG. 5. The empirically determined Cr–O phase diagram. Different symbols are used to group data points according to growth morphology (epi =epitaxial, poly=polycrystalline, and amorphous) and oxidation state.

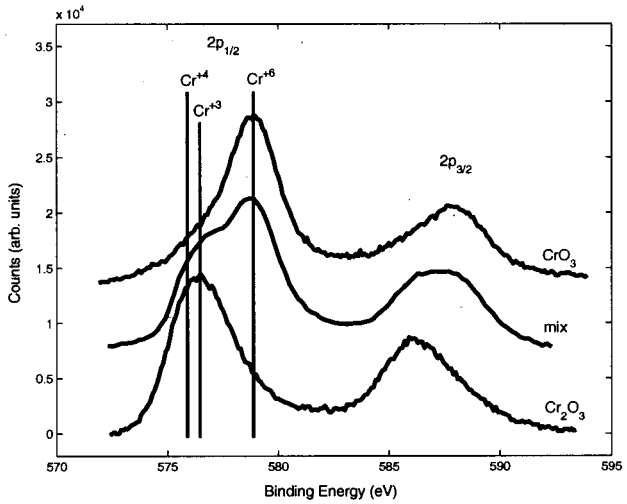

FIG. 6. Cr $2p$ *in situ* core level x-ray photoemission indicating the chemical shift due to oxidation state.

with a constant Cr deposition rate of 0.5 Å/s. As seen for Mo and W, there is a sublimation region at higher temperature and oxidation potential. However, in this case the oxidation state of the small amount of Cr detected via XPS was either $+3$ and or $+6$. No correlation was found between the temperature or oxidation potential and the oxidation state of this thin layer of oxidized Cr. The one striking difference the Mo and W phase diagrams and that of Cr is that the oxidation state of Cr does not change abruptly. On moving up in oxidation potential from the Cr_2O_3 region, a large region in phase space is encountered with mixed oxidation states. Figure 5 shows a set of Cr core level XPS results. The top and bottom curves are for CrO_3 and Cr_2O_3, respectively. The middle curve, obtained from growth conditions of 200 °C and an atomic oxygen flux of 2×10^{17} atoms/cm^2 s, shows a mix of the $+3$, $+4$, and $+6$ oxidation states, CrO_2, Cr_2O_3, and CrO_3, respectively. Because the largest peak asymmetries associated with core-level photoemission are on the higher binding energy side of the peak and the chemical shift for Cr in the $+4$ oxidation state puts the CrO_2 peak at the lowest binding energy, we can fairly easily determined whether the $+4$ oxidation state is present. We have used three slightly different techniques to approximately determine the amount of each phase present. Fitting the leading edge (lower binding energy edge) of the spectra with a set of Gaussian curves, fitting the full spectra with a set of Voigt curves, and fitting the full spectra with the experimentally determined spectra for the Cr_2O_3 and CrO_3, while assuming the remaining spectra weight is due to CrO_2, all suggest that the sample composition is approximately 5% CrO_2, 30% Cr_2O_3, and 65% CrO_3. As temperature and oxidation potential are varied in the central mixed oxidation state region of the phase diagram the amount of CrO_2 remains small but fairly constant while the ratio of Cr_2O_3 to CrO_3 changes according to the proximity to the single phase regions.

We have also tried to obtain CrO_2 via decomposition of the CrO_3 films *in situ*. Heating to 150 °C in vacuum (1×10^{-9} Torr) indicates decomposition occurs directly to Cr_2O_3, with at most 5% CrO_2. The core-level XPS of these heat treated films looks identical to the XPS spectra form the mixed phase region (see Fig. 6).

It has routinely been shown that by growing epitaxial films on a well matched substrate, a ''better'' single-crystal-like film can be grown. It is also commonly believed that by using a substrate with a matched structure and lattice parameters, the growth of a particular phase, which may not grow otherwise, can be enhanced. In this article we used both TiO_2 or Al_2O_3 substrates for all the film growths and found no dependence on the substrate used to either grow a particular phase, or grow a single-crystal-like film. Cr_2O_3 grew single crystal-like on TiO_2 substrates, and MoO_2, MoO_3, WO_2, and WO_3 all grew single crystal-like on both TiO_2 and Al_2O_3. the amount of CrO_2 found in the mixed oxidation region of the Cr–O phase diagram was not enhanced by the use of a TiO_2 substrate, the closest matching substrate that is readily available.

IV. CONCLUSION

In summary, the use of our high-flux atomic oxygen source significantly increases the temperature–oxidation potential parameter space that we can search for appropriate growth conditions of CrO_2 using MBE-like techniques. Within this enlarged parameter space we did not find suitable growth conditions for single phase CrO_2. At extreme oxidation potentials we are able to grow CrO_3, a higher oxidation state, suggesting that we can generate more than enough oxygen to oxidize Cr. Comparisons with the Mo and W phase diagrams suggest that single phase regions are found next to the sublimation region, which we studied carefully in the Cr phase diagram, and also that the temperatures required for the Cr oxides to stick to the substrate may be too low for kinetics to allow a single oxidation state to be present. The potential for epitaxial growth of CrO_2 on structurally matched TiO_2 substrates did not enhance the ability grow single phase CrO_2. More generally, we find that low pressures of activated oxygen cannot always be use as a direct

replacement for higher pressures of molecular oxygen. One possible interpretation of these results is that even though we have the oxidation potential, via our high flux atomic oxygen source, to drive Cr up to and past the +4 oxidation state we still cannot form CrO_2 because the physical effect of pressure may be significant for driving the kinetics associated with forming the rutile structure for Cr and O, and hence required to form CrO_2. It is worth pointing out that the only low pressure technique currently available for growing CrO_2, the simple two-zone atmospheric pressure CVD growth method, can be understood by recognizing the need for the intermediate state Cr_8O_21.[25] The presence of this intermediate state can be considered to open a kinetic pathway for the formation of CrO_2 that is not normally accessible at low pressures.

ACKNOWLEDGMENTS

This work was supported by the NSF though the Stanford MRSEC program, and by the Air Force Office of Scientific Research.

[1] A. M. Bratkovsky, Phys. Rev. B **56**, 2344 (1997).
[2] H. Y. Hwang and S.-W. Cheong, Science **278**, 1607 (1997).
[3] S. S. Manoharan, D. Elefant, G. Reiss, and J. B. Goodenough, Appl. Phys. Lett. **72**, 984 (1998).
[4] J. M. D. Coey, A. E. Berkowitz, Ll. Balcells, F. F. Putris, and A. Barry, Phys. Rev. Lett. **80**, 3815 (1998).
[5] A. M. Bratkovsky, Appl. Phys. Lett. **72**, 2334 (1998).
[6] M. A. Korotin, V. I. Anisimov, D. I. Khomskii, and G. A. Sawatzky, Phys. Rev. Lett. **80**, 4305 (1998).
[7] R. C. DeVries, Mater. Res. Bull. **1**, 83 (1966).
[8] L. Ranno, A. Barry, and J. M. D. Coey, J. Appl. Phys. **81**, 5774 (1997).
[9] S. Ishibashi, T. Namikawa, and M. Satou, Jpn. J. Appl. Phys. **17**, 249 (1978).
[10] S. Ishibashi, T. Namikawa, and M. Satou, Mater. Res. Bull. **14**, 51 (1978).
[11] K. Suzuki and P. M. Tedrow, Phys. Rev. B **58**, 11 597 (1998).
[12] X. W. Li, A. Gupta, T. T. McGuire, P. R. Duncombe, and G. Xiao, J. Appl. Phys. **85**, 5585 (1999).
[13] X. W. Li, A. Gupta, and G. Xiao, Appl. Phys. Lett. **75**, 713 (1999).
[14] A. Barry, J. M. D. Coey, and M. Viret, J. Phys.: Condens. Matter **12**, L173 (2000).
[15] N. J. C. Ingle, R. H. Hammond, M. R. Beasley, and D. H. A. Blank, Appl. Phys. Lett. **75**, 4162 (1999).
[16] D. A. Shirley, Phys. Rev. B **5**, 4709 (1972).
[17] W. Tilk and W. Klemm, Z. Anorg. Allg. Chem. **240**, 355 (1939).
[18] T. Fujii, F. M. F. de Groot, G. A. Sawatzky, F. C. Voogt, T. Hibma, and K. Okada, Phys. Rev. B **59**, 3195 (1999).
[19] G. H. Smudde, Jr. and P. C. Stair, Surf. Sci. **317**, 65 (1994).
[20] T. Jirsak, M. Kuhn, and J. A. Rodriguez, Surf. Sci. **457**, 254 (2000).
[21] N. Beatham, P. A. Cox, R. G. Egdell, and A. F. Orchard, Chem. Phys. Lett. **69**, 479 (1980).
[22] A. Gulino, S. Parker, F. H. Jones, and R. G. Egdell, J. Chem. Soc., Faraday Trans. **92**, 2137 (1996).
[23] E. Fromm, E. Gebhardt, Editors, *Reine unde Angewandte Metallkunde in Einzeldarstellungen*, Gase und Kohlenstoff in Metallen, Vol. 26 (Springer, New York, 1976).
[24] I. Barin, *Thermochemical Data of Pure Substances*, 3rd ed. (VCH, New York, 1995).
[25] P. G. Ivanov, S. M. Watts, and D. M. Lind, J. Appl. Phys. **89**, 1035 (2001).